Journal of Catalysis **185,** 378–385 (1999)
Article ID jcat.1999.2475, available online at http://www.idealibrary.com on IDEAL®

Characterization and Catalytic Properties of Hydrothermally Dealuminated MCM-22

P. Mériaudeau,[1] Vu A. Tuan, Vu T. Nghiem, F. Lefevbre,* and Vu T. Ha

*IRC/CNRS, 2 Avenue Albert Einstein, 69626 Villeurbanne, France; and *COMS/CPE, Université Claude Bernard, 43, Boulevard du 11 Novembre, 69626 Villeurbanne, France*

Received November 26, 1998; revised February 11, 1999; accepted March 6, 1999

MCM-22 has been synthesized and dealuminated by hydrothermal treatments. The resulting solids were characterized by different techniques in order to know how the acid properties of the dealuminated solids were modified. It appears that the number of acid sites was decreased by hydrothermal treatments but the acid strength was not modified. Nondealuminated and dealuminated solids were used in the *n*-octane hydroconversion. Results suggested that for both types of solids the hydroisomerization is mainly occurring in the 10-membered ring (MR) channels whereas the hydrocracking is mainly coming from acid sites located in 12-membered ring channels. According to the observed distribution of monobranched isomers, MCM-22 shows some "shape-selective" character typical of the pentasil family, whereas, according to the absolute yield of isopentane in the hydrocracked products at low hydrocracking conversions, "MCM-22 behaves more like a 12 MR zeolite" (6). Similar conclusions were proposed in (7).

Key Words: **MCM-22; dealumination; hydroconversion.**

INTRODUCTION

Zeolite MCM-22 was recently patented as a useful catalyst for alkylation and isomerization reactions and for conversion of methanol or olefins to hydrocarbons (1–3). More recently, it has been shown that the porosity of MCM-22 is composed of two independent 10-ring channels, with one of these channels containing large supercages of 12-ring (4, 5). From *n*-decane hydroisomerization studies (6, 7) it was concluded that MCM-22 presents shape-selective properties of both 10- and 12-membered ring (MR) zeolites, depending on the particular criterion used: according to the observed distribution of monobranched isomers, MCM-22 shows some "shape-selective" character typical of the pentasil family, whereas, according to the absolute yield of isopentane in the hydrocracked products at low hydrocracking conversions, "MCM-22 behaves more like a 12 MR zeolite" (6). Similar conclusions were proposed in (7).

[1] To whom correspondence should be addressed.

$SiCl_4$ treatments (8) or hydrothermal treatments (9) have been shown as an effective way to dealuminate the zeolite framework. The dealumination studies were performed in order to remove most of the Al in the framework and as a consequence to have a much better resolution for the ^{29}Si NMR spectrum. Using this procedure, the authors were able to distinguish experimentally seven distinct Si sites.

Succinct characterization of the acidity of the dealuminated and nondealuminated solids was reported (5–10); Brønsted acid sites were observed by using IR spectroscopy ($\nu_{OH} = 3620\ cm^{-1}$), all of which were accessible for pyridine (10).

The aim of this work is to report on the hydrothermal dealumination of MCM-22 and its effect on the acidity and on the catalytic properties in *n*-octane hydroconversion.

EXPERIMENTAL

Zeolite Synthesis and Dealumination

The zeolite synthesis conditions used here are the same as those described earlier (11): 0.55 g of $NaAlO_2$ (Carlo Erba) and 0.59 g of NaOH were dissolved in 60 g of H_2O. To this solution, 6 g of silica (Degussa), 0.16 g of H_2SO_4, and 10 g of H_2O were added under stirring; finally, 3.6 g of hexamethyleneimine (Aldrich) and 10 g of H_2O were added. The resulting gel was introduced into a PTFE-lined stainless-steel autoclave rotated at 60 rpm and heated at 423 K for 11 days. To remove the template, the synthesized solid was calcined for 48 h at 810 K under nitrogen containing 5 vol% oxygen.

The ammonium form was prepared via a threefold ion exchange at 350 K with a 1 N aqueous solution of NH_4Cl. This batch was used to prepare dealuminated samples.

The parent zeolites were hydrothermally dealuminated at different temperatures, H_2O pressure being fixed at 10 kPa. The sample was loaded in a dynamic microflow reactor (1 g of sample) and heated under a flow of N_2 at the desired temperature and then N_2 was replaced by ($N_2 + H_2O$): 773 K for D 773 MCM-22 for 2 h, 973 K for D_2 973 MCM-22 for 3 h, and 973 K for D_3 973 MCM-22 for 3 days.

0021-9517/99 $30.00

Characterization

The ^{13}C, ^{27}Al, ^{29}Si MAS-NMR spectra were recorded on a Bruker DSX-300 spectrometer. Chemical shifts were referenced to the classical external standards: TMS for Si and $[Al(H_2O)_6]^{3+}$ for Al. Cross-polarization was used for ^{13}C. ^{27}Al MAS-NMR spectra were obtained using a pulse length of 1 μs ($\pi/6$) and a recycle delay of 1 s.

The chemical composition of the MCM-22 (H form) was determined by AES (atomic emission spectroscopy).

The X-ray powder diffraction (XRD) patterns were obtained with a Philips W1050 powder diffraction spectrometer. The samples were stored in a desiccator, in the presence of water at ambient temperature for 2 days before registration of X-ray diffraction patterns.

Morphology and particle sizes were estimated from scanning electron microscopy (Hitachi S800 apparatus). IR spectra were recorded with Perkin-Elmer 580 FT IR spectrometer; the solids were pressed in small wafers (~20 mg) and activated after having been mounted in a special IR cell allowing thermal treatments under controlled atmosphere.

Catalytic Tests

The *n*-octane hydroisomerization was studied over nondealuminated and dealuminated solids. For this purpose, the supports were loaded with 0.5 wt% Pt and 1 wt% Pd (wet impregnation technique); the metal precursors were $Pt(NH_3)_4(OH)_2$ and Pd $(NH_3)_4(OH)_2$ (Johnson Matthey). Solids were calcined under an oxygen flow from room temperature to 573 K for 12 h, flushed with nitrogen, and then reduced under a flow of hydrogen, with the temperature increased to 773 K (ramping 1 K/min). After 4 h at this temperature, the temperature was decreased to 523 K.

The reaction was carried out in a fixed-bed flow reactor working at atmospheric pressure, temperature being fixed at 523 K. The H_2/C_8 molar ratio was 54 and the space velocity was varied from 0.5 to 8 h^{-1} in order to vary the conversion.

Reactant and products were analyzed by gas chromatography, chromatographs being equipped with a capillary Pona column and with a Unibed column (both from Altech, France). For all solids, the metal-loaded catalysts were checked to ensure that they are true bifunctional catalysts: among the cracked products C_1 and C_2 are in negligible amounts and the *n*-octane conversion varied as the inverse of the hydrogen pressure (see Catalytic Results).

RESULTS

Chemical Analysis

Si/Al (atomic) was found close to the expected value (15.4 compared to 15). The XRD pattern of the calcined sample is

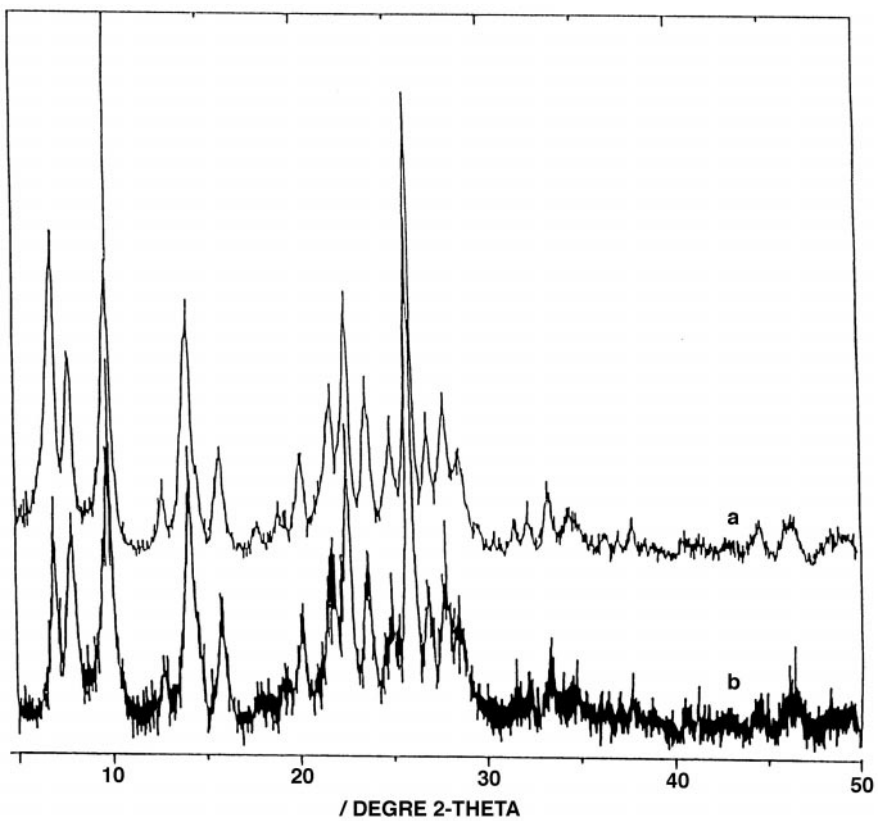

FIG. 1. XRD patterns of (a) MCM-22 and (b) D_3 973 MCM-22.

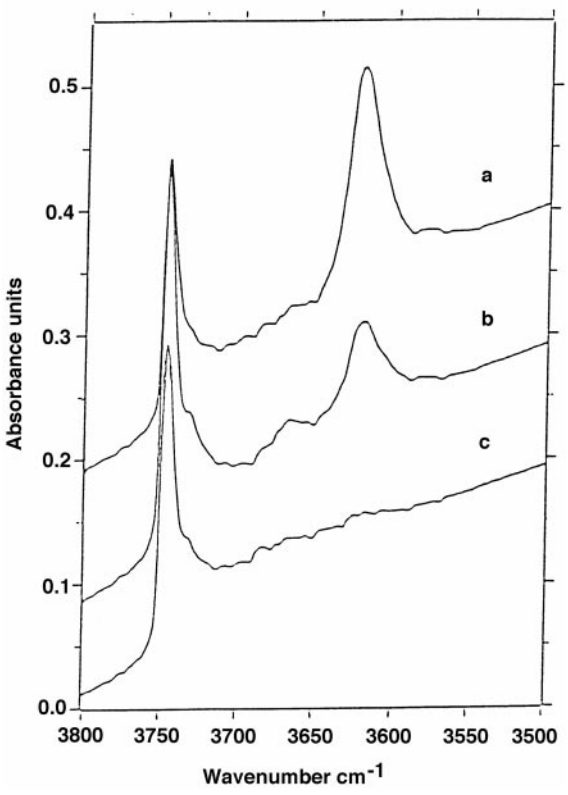

FIG. 2. Infrared spectra of MCM-22 (a), D 773 MCM-22 (b), and D_2 973 MCM-22 (c).

given in Fig. 1. It appears that the diffractogram is identical to that expected for an MCM-22 structure (4) and no other X-ray line due to impurity is observed.

On the same figure the XRD pattern obtained for the highly dealuminated sample D_3 973 MCM-22 is given. Again the MCM-22 structure is still present but a reduced intensity of the different lines suggests that a loss of crystallinity has occurred.

SEM

The MCM-22 zeolite is composed of thin plates having different morphologies with the largest dimension close to 0.5 μm and the thickness less than 0.1 μm. The same morphologies were reported previously (5, 11).

IR Results

IR studies were performed on the nondealuminated ammonium-exchanged MCM-22 and on two dealuminated MCM-22 samples.

Before registration of the IR spectrum, the sample was first thermally treated at $T = 773$ K for 12 h under vacuum.

The spectra recorded for the three samples under study are given in Figs. 2a (MCM-22), 2b (D 773 MCM-22), and 2c (D_2 973 MCM-22).

In these figures, three different vibrations are observed at 3747, 3664, and 3622 cm^{-1}. These vibrations are attributed to silanols groups (3747 cm^{-1}), Al–OH (Al belonging to extraframework Al, see below), and Si(OH)Al Brønsted acid sites (11). Figure 2a indicates that the MCM-22 already contains extraframework Al before dealumination treatment; this is attributed to partial dealumination during the template removal as suggested by Corma *et al.* (11). Comparison among Figs. 2a–2c indicates that the absorbance of the vibration at 3622 cm^{-1} is decreasing when the severity of the hydrothermal treatment is increasing. This result suggests that part of framework Al is extracted because of the hydrothermal treatment and by consequence causes a decrease in Si(OH)Al group concentration.

Figures 2 also indicates a change of the absorbance of vibration at 3664 cm^{-1} with the hydrothermal treatment: an increase of this vibration is observed for D 773 MCM-22 compared to MCM-22. This increase is due to the extraction of framework Al forming highly dispersed extraframework Al. A more severe dealumination causes a decrease of both vibrations at 3622 and 3664 cm^{-1}; the decrease of the number of OH groups linked to extraframework Al is probably due to the growth of Al_2O_3 extraframework particles.

In order to characterize the OH groups described above, pyridine was adsorbed at RT and desorbed at increasing temperatures. Figures 3 and 4 show the vibrations observed

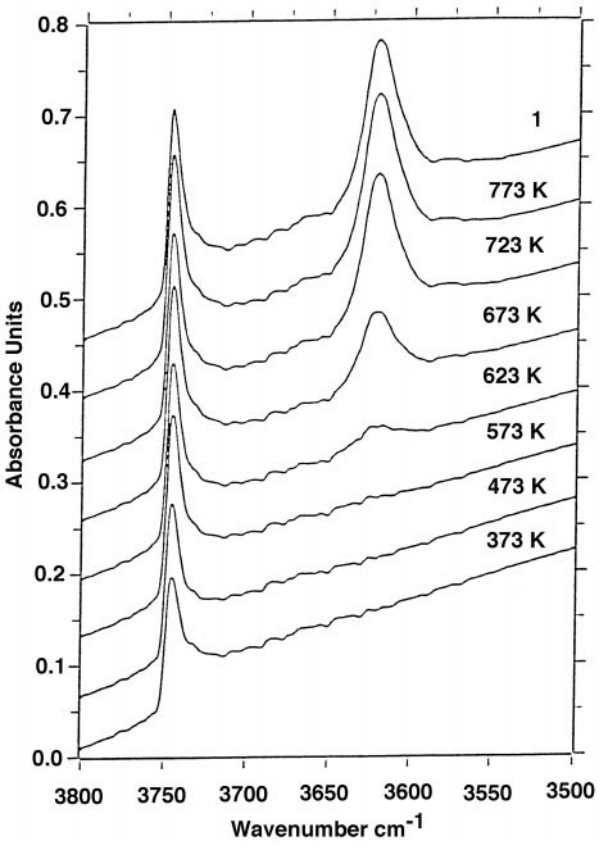

FIG. 3. Infrared spectra (3800–3500 cm^{-1}) of MCM-22 after pyridine adsorption and desorption at increasing temperatures (1) before pyridine adsorption.

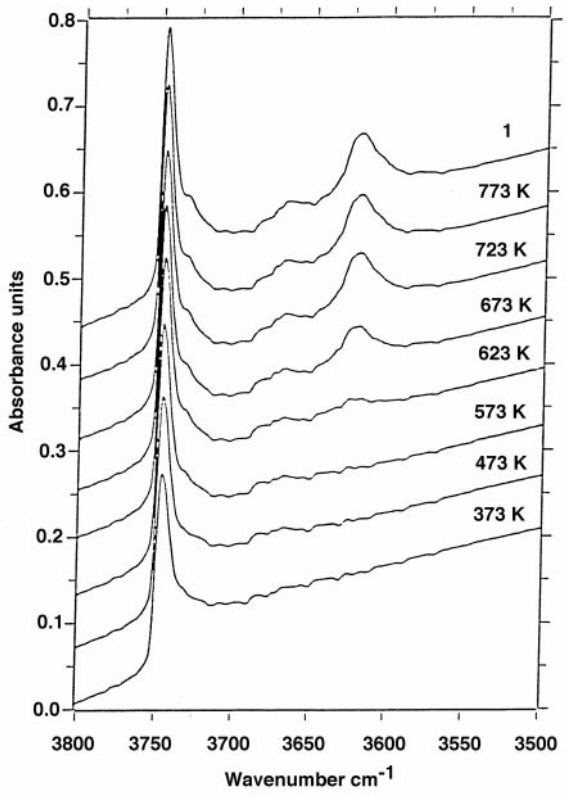

FIG. 4. Infrared spectra (3800–3500 cm^{-1}) of D 773 MCM-22 after pyridine adsorption and desorption at increasing temperatures (1) before pyridine adsorption.

in the range 3800–3500 cm^{-1} and Figs. 5–7 for the vibrations in the 1700–1400 cm^{-1} range.

The pyridine adsorption causes the complete vanishing of Brønsted acid sites vibrating at 3622 cm^{-1} and a nearly complete vanishing of the vibration at 3664 cm^{-1}.

Figures 5–7 show that upon pyridine adsorption some vibrations appeared (1700–1400 cm^{-1} range): IR bands at 1540 and 1450 cm^{-1} are characteristics of pyridinium ions and of pyridine coordinatively bonded to Lewis acid sites, respectively (11).

For all samples, it is observed that the desorption of pyridine at increasing temperatures causes a strong decrease of the vibrations at 1540 and 1450 cm^{-1} and that initial OH vibrations at 3622 and 3664 cm^{-1} are partially restored. A careful examination of Fig. 4 indicates that for pyridine desorption at 573 K, the OH vibrations at 3664 cm^{-1} are fully restored whereas OH vibrations at 3622 cm^{-1} are not observed. This result indicates that the acid strength of Brønsted OH groups vibrating at 3664 cm^{-1} is weaker than that of the OH groups vibrating at 3622 cm^{-1}. From this observation, it can also be deduced that the pyridinium ions still existing after desorption at 573 K are exclusively due to pyridine having reacted with OH groups at 3622 cm^{-1}.

From Figs. 5–7, one can also deduce the change in the pyridine ion absorbances as a function of desorption temperature. This has been plotted in Fig. 8 which indicates that for nontreated MCM-22 and D 773 MCM-22 the disappearance of pyridinium ions follows the same trend whereas this disappearance occurs at a lower temperature for D_2 973 MCM-22. In other words, the acid strength of OH groups ($\nu_{OH} = 3622\ cm^{-1}$) for MCM-22 and D 773 MCM-22 samples is the same, while that of D_2 973 MCM-22 is weaker.

NMR Results

The ^{13}C CP-MAS-NMR spectrum of the as-synthesized MCM-22 displays numerous peaks at 26.8, 47.5, 56.4, ca 130, and 163.4 ppm. If some of these peaks can be attributed to hexamethyleneimine and to the corresponding cation, other peaks cannot be due to these species. In particular, the peaks at 130 and 163.4 ppm can only be assigned to *sp*2 carbon atoms coordinated or not to nitrogen via a double bond. Even if these species are in a minor amount, they show that during the synthesis a partial dehydrogenation of the template occurred.

The ^{27}Al MAS-NMR spectrum of the as-synthesized sample shows only one signal at 54 ppm with a shoulder at ca 50 ppm corresponding to tetrahedrally coordinated

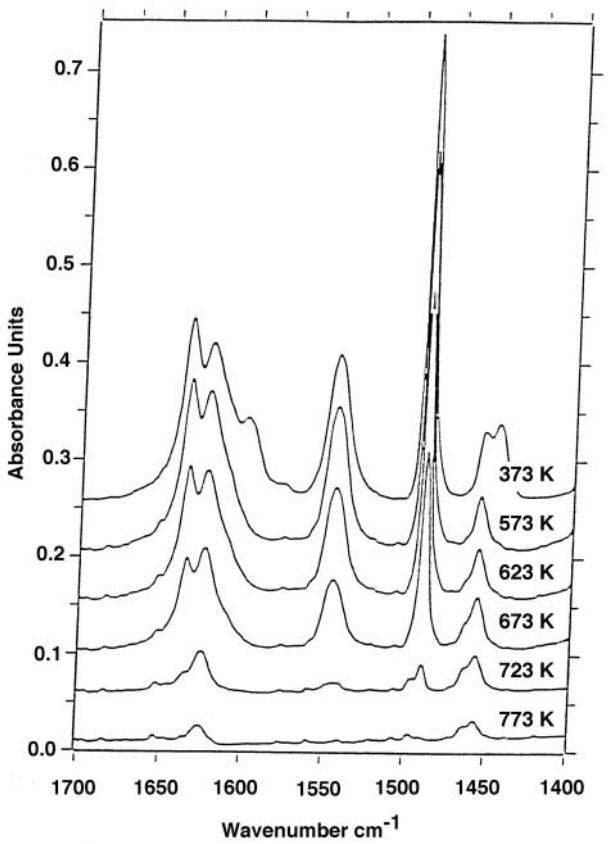

FIG. 5. Infrared spectra (1700–1400 cm^{-1}) of MCM-22 after pyridine adsorption and desorption at increasing temperatures.

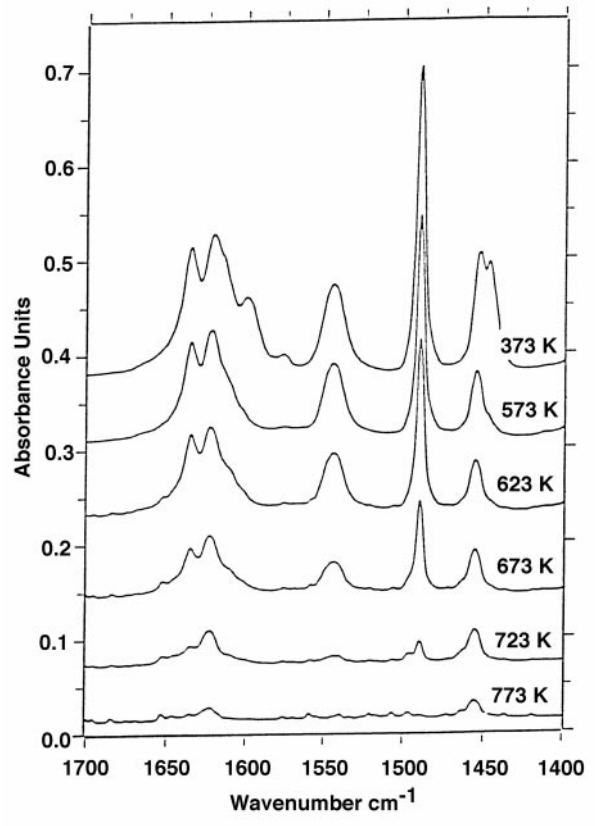

FIG. 6. Infrared spectra (1700–1400 cm^{-1}) of D 773 MCM-22 after pyridine adsorption and desorption at increasing temperatures.

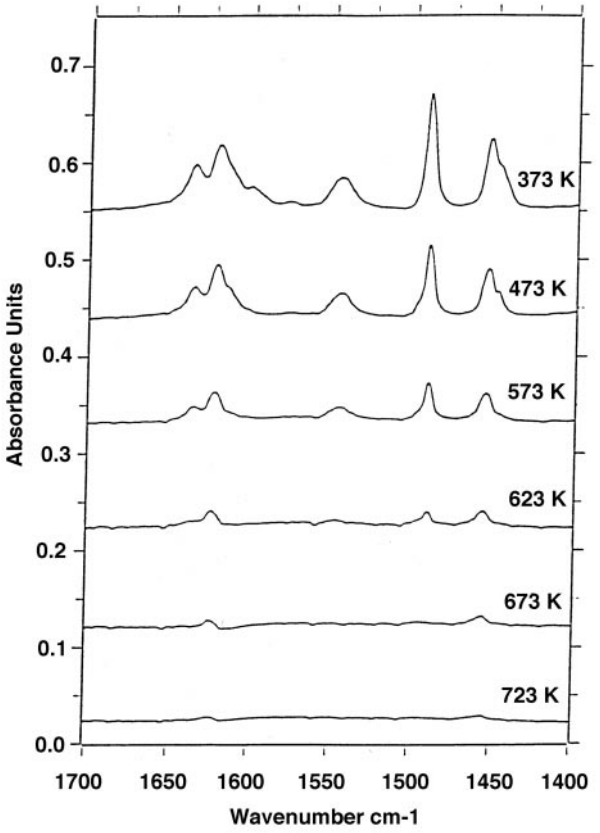

FIG. 7. Infrared spectra (1700–1400 cm^{-1}) of D_2 973 MCM-22 after pyridine adsorption and desorption at increasing temperatures.

aluminum in the framework of the MCM-22 sample (Fig. 9). After calcination a new sharp peak appears at 0 ppm corresponding to isolated aluminum ions in an octahedral coordination, located outside the framework. After dealumination at 773 K the ^{27}Al NMR spectrum has slightly changed: the intensity of the peak at 0 ppm has increased, while the shape of the peak corresponding to the tetrahedral aluminum atoms has been modified; the shoulder has increased compared to the signal at 54 ppm and now has the same intensity. After dealumination at 973 K for 3 h, the spectrum becomes broader: the sharp peak at 0 ppm is now broadened, due to the formation of polymeric octahedral aluminum atoms as in alumina. The signal at 54 ppm has completely disappeared and has been replaced by a broad signal centered at ca 48 ppm. One can also think that there is a broad signal at ca 30 ppm due to extraframework aluminum in a tetra- or pentacoordinate. After dealumination at 973 K for 3 days the broadening of the peaks has increased and the peak corresponding to tetrahedral aluminum atoms in the framework has continued to shift to lower ppm. One can now distinguish two peaks at ca 49 and 39 ppm.

These results show the following:

(1) If in the as-synthesized material there is no extraframework aluminum, the calcination leads to the formation of some isolated octahedral aluminum species, responsible of the infrared band at 3664 cm^{-1}.

(2) Dealumination at 773 K increases the number of these extraframework aluminum atoms without sensible aggregation.

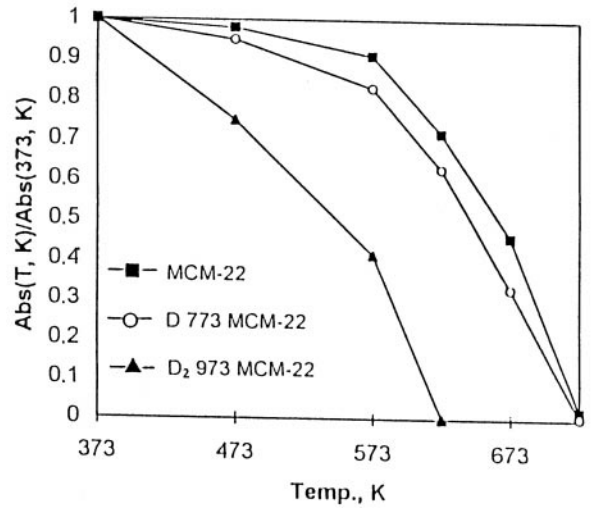

FIG. 8. Change in relative pyridium ion absorbances for different samples at increasing desorption temperatures.

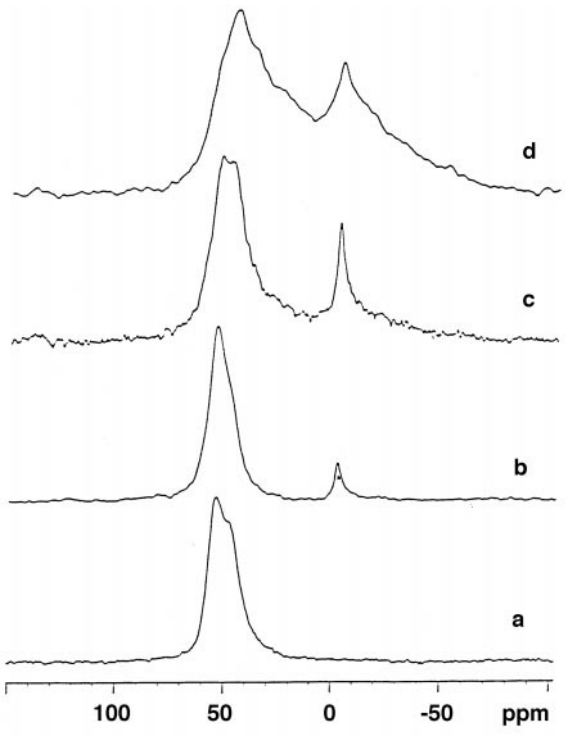

FIG. 9. ^{27}Al MAS-NMR spectra of (a) as-synthesized MCM-22, (b) MCM-22 after calcination, (c) D 773 MCM-22, and (d) D_2 973 MCM-22.

(3) Dealumination at 973 K results in an aggregation of the octahedral extraframework aluminum atoms, leading then to a decrease of the corresponding Al–OH groups.

(4) The chemical shift of the aluminum atoms in the framework decreases when the dealumination is more important. Such an effect is well known in the literature but in our case the variation is more important as the chemical shift varies from 54 to 39 ppm. This decrease is probably related to the increasing distortion around the aluminum atom when the Si/Al (framework) ratio increases. These results show that the attribution previously made of the peak at ca 30 ppm in dealuminated species to a distorted tetrahedral aluminium atom is probably true. However, our results show that such a species can be found in the framework when the Si/Al (framework) ratio is very high.

The ^{29}Si MAS-NMR spectra of the various samples are given in Fig. 10. The spectrum of the initial material shows only three relatively broad signals between −103 and −120 ppm. New peaks appear when the Si/Al ratio increases and in the final material one can easily distinguish sharp peaks at −108, −113.7, −116.2, and −120.2 ppm with the same intensity and the same linewidth and a relatively broad signal between −111 and −113 ppm with two shoulders and corresponding probably to the sum of three components. This spectrum is quite similar to that reported in (11) for the ITQ-1 zeolite or in (9) for highly dealuminated MCM-22.

Catalytic Results

The reaction of *n*-octane produced cracked products (C_3–C_5) and C_8 isomers. Among the cracked products, C_1 and C_2 are in trace amounts, indicating that the hydrogenolysis reaction over metal function was negligible. For both samples studied it has been checked by varying H_2/HC ratios that the metal and acid functions are well balanced and that Pt–Pd MCM-22 behaves like a true bifunctional catalyst (13).

In Fig. 11 is reported the isomerization yield versus *n*-octane conversion. The isomerization selectivity as well the selectivity toward monomethyl isomers is also reported. It appears that even for low conversion the isomerization selectivity reached was relatively low. In Table 1 the product distribution obtained at low conversion for non dealuminated and dealuminated MCM-22 is listed. Figure 11 and Table 1 show clearly that the catalytic behavior of MCM-22 was considerably modified upon dealumination.

It is known from the literature that MCM-22 porosity is composed of two nonintersecting porous systems, one

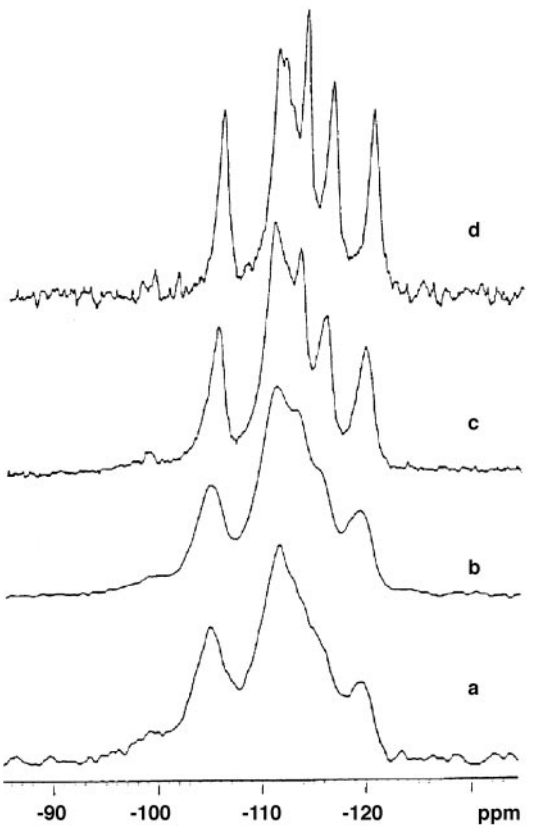

FIG. 10. ^{29}Si MAS-NMR spectra of (a) as-synthesized MCM-22, (b) MCM-22 after calcination, (c) D 773 MCM-22, and (d) D2 973 MCM-22.

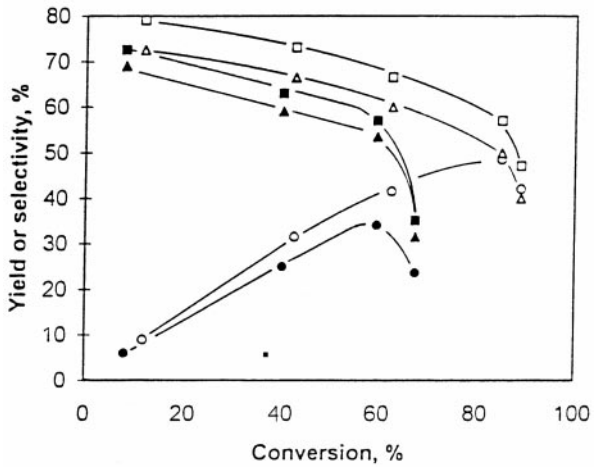

FIG. 11. Reaction of *n*-octane: change in isomerization yield (○), isomerization selectivity (□), and monomethyl isomer selectivity (△) versus conversion. Open symbols, MCM-22; black symbols, D 773 MCM-22.

having a 10-T ring and the other a 10-T ring channel with pockets of 12-T rings (4).

It is also known from the literature that the linear alkanes are very selectively hydroisomerized over 10-membered ring pore zeolites like ZSM-22 (14), ZSM-23 (15), and ZSM-48 (16) or medium pores SAPOs (SAPO-11, SAPO-31, and SAPO-41(17) (18)): at high conversions (80–90%) the hydroisomerization selectivity was always very high. The pore architecture of MCM-22 which is constituted, as stated above, by 10- and 12-membered ring channels, was further derived from study of the *n*-decane reaction (6, 7).

The results we have obtained for *n*-octane hydroconversion also reveal that the catalytic behavior of MCM-22 is complex: from Table 1 it is observed that the iC_4/C_4 ratio is close to that obtained for large molecular pore sieves such as SAPO-5 (19) but different from that obtained for 10-membered ring zeolites; the same remark is true when considering the $(C_3 + C_5)/C_4$ ratio. These results suggest that the contribution to hydrocracking of surface acid sites and/or of acid sites located in large pores having 12-membered rings is larger than that of acid sites located in 10-membered rings.

TABLE 1

***n*-Octane and $2MC_7$ Hydroconversion (Distribution of Products Obtained at Low Conversion (10%))**

	n-Octane					$2MC_7$
Reactants/solid	IC_4/C_4	$\frac{iC_5}{C_5}$	$\frac{C_3+C_5}{C_4+iC_4}$	$\frac{2MC_7}{3MC_7}$	$\frac{2-5DMC_6}{2-4DMC_6}$	$3MC_7/n\text{-}C_8$
MCM-22	1.75	10	0.86	1.6	3	1.15
D 773 MCM-22	1.65	7	0.88	1.8	3.2	1.10
SAPO-5[a]	2.4	6	0.87	0.8	0.85	8
ZSM-23[b]	0.93	1.9	1.1	2.1	2.2	0.8

[a,b] From Ref. (19).

By contrast, the high values obtained for $2MC_7/3MC_7$ and 2–5 DMC_6/2–4 DMC_6 indicated that for hydroisomerization the contribution of pores with large pockets is negligible. In line with this conclusion is the low value of the $3MC_7/n\text{-}C_8$ ratio obtained with $2MC_7$ as a reactant (19). Apparently those C_8 molecules reaching 12-membered ring channels were preferentially cracked while those in 10-membered rings were preferentially isomerized.

Due to the peculiar shape of pores having 12-ring pockets (these pockets are linked via 10-ring apertures (5)) it can be assumed that *n*-octane will be able to enter in such pores and be transformed in these large pockets into MC_7, DMC_6, and TMC_5. MC_7, DMC_6, and TMC_5 isoolefins in the large pockets would have to diffuse across 10-ring apertures. Highly branched isomers will be formed and cracked into iC_4 and possibly C_4 and $C_3 + iC_5$ (and/or C_5). Thus most of the cracked products will reflect the contribution of pores with large pockets.

The results of Table 1 also indicated that the contribution of surface acid sites and/or of acid sites located at the pore mouth of pores with 12-membered pockets is negligible as compared to that of all acid sites because the $3MC_7/n\text{-}C_8$ ratio obtained with $2MC_7$ as a feed clearly indicates a shape-selectivity effect (19). This could be due to a small number of surface acid sites as compared to the total number of acid sites and/or to their small intrinsic activity due to their location.

The results obtained with MCM-22 and D_2 973 MCM-22 indicated that the isomerization yield is lower on dealuminated solid. Within the cracked products formed the distribution of light alkanes (C_3–C_5) was not deeply modified by dealumination, indicating that the explanation proposed above for MCM-22 is still valid for D 773 MCM-22. The slight increase of the $2MC_7/3MC_7$ ratio with *n*-octane as a feed and of $n\text{-}C_8/3MC_7$ with $2MC_7$ as a feed suggests that the porosity constraint is reinforced by dealumination. This reduced porosity of 10-membered ring pores could be due to the extraction of aluminum of the framework and its deposit as very small alumina debris, inside the channels.

Finally, it is observed that at high conversion ($\alpha > 60\%$) over MCM-22 and D 773 MCM-22, the isomerization yield is decreased as expected: this phenomenon is general for large-pore zeolites were the dimethyl and trimethyl intermediates formed in large amount due to the lack of spatial constraint, these products being hydrocracked to form C_4, C_3, and C_5 alkanes.

CONCLUSIONS

MCM-22 zeolite has been synthesized and dealuminated by hydrothermal treatments. Dealumination treatment causes a decrease in the number of Brønsted acid sites but the acid strength is not modified as observed by pyridine TPD studies for MCM-22 and D 773 MCM-22.

For highly dealuminated zeolite D_2 973 MCM-22, the acid strength of Brønsted acid sites is weaker.

Studies of *n*-octane hydroconversion indicate that most of the hydroisomerization products are formed in 10-T-membered ring channels whereas the hydrocraking is mainly occurring on acid sites located in 12-membered ring channels. Comparison of product distribution between MCM-22 and dealuminated MCM-22 suggested that aluminum debris located in the porosity reinforced the shape selectivity.

REFERENCES

1. Huss, A., Kirker, G. W., Keville, K. M., and Thomson, R. T., U.S. Patent 4 992 615, 1991.
2. Del Rossi, K. J., and Huss, A., U.S. Patent 5 107 047, 1992.
3. Chu, C. T., U.S. Patent 4 956 514, 1990.
4. Leonowicz, M. E., Lawton, J. A., Lawton, S. L., and Rubin, M. K., *Science* **264**, 1910 (1994).
5. Lawton, S. L., Leonowicz, M. E., Partridge, R. D., Chu, P., and Rubin, M. K., *Microporous Mesoporous Mater.* **23**, 109 (1998).
6. Corma, A., Corell, C., Llopis, F., Martinez, A., and Perez-Pariente, J., *Appl. Catal. A* **115**, 121 (1994).
7. Souverijns, W., Verrelst, W., Vanbustsele, G., Martens, J. A., and Jacobs, P. A., *J. Chem. Soc. Chem. Commun.*, 1671 (1994).
8. Hunger, M., Ernst, S., and Weitkamp, J., *Zeolites* **15**, 188 (1995).
9. Kennedy, G. J., Lawton, S. L., and Rubin, M. K., *J. Am. Chem. Soc.* **116**, 11000 (1994).
10. Corma, A., Corell, C., Fornés, V., Kolodziejski, W., and Perez-Pariente, J., *Zeolites* **15**, 576 (1995).
11. Corma, A., Corell, C., and Perez-Pariente, J., *Zeolites* **15**, 2 (1995).
12. Camblor, M. A., Corma, A., and Dias-Cabanas, M. J., *J. Phys. Chem. B* **102**, 44 (1998).
13. Mériaudeau, P., Tuan, Vu. A., Lefebvre, F., Nghiem, Vu. T., and Naccache, C., *Microporous Mesoporous Mater.*, in press.
14. Martens, J. A., Parton, R., Uytterhoeven L., Jacobs, P. A., and Froment, G., *Appl. Catal.* **76**, 95 (1991).
15. Ernst, S., Kumar, R., and Weitkamp, J., *Catal. Today* **3**, 1 (1988).
16. Mériaudeau, P., Tuan, Vu. A., Nghiem, Vu. T., Sapaly, G., and Naccache, C., *J. Catal.* **185**, 435 (1999).
17. Miller, S. J., U.S. Patent 5, 135, 638 (1992).
18. Miller, S. J., *Microporous Mater.* **2**, 439 (1994).
19. Mériaudeau, P., Tuan, Vu. A., Sapaly, G., Nghiem, Vu. T., and Naccache, C., "12th International Zeolite Conference, Baltimore, July 5–10 1998," in press.